2-2010

Liquid Filled Microstructured Optical Fiber for X-Ray Detection

S. L. DeHaven

S. Albin
Old Dominion University

W. C. Kelliher

Liquid filled microstructured optical fiber for x-ray detection

S. L. DeHaven,[1,*] S. Albin,[2] and W.C. Kelliher[1]

[1]NASA Langley Research Center, Hampton, VA 23681, USA
[2]Old Dominion University, Norfolk, VA.23508, USA
[*]stanton.l.dehaven@nasa.gov

Abstract: A liquid filled microstructured optical fiber (MOF) is used to detect x-rays. Numerical analysis and experimental observation leads to geometric fiber optics theory for MOF photon transmission. A model using this theory relates the quantity and energy of absorbed x-ray photons to transmitted MOF generated photons. Experimental measurements of MOF photon quantities compared with calculated values show good qualitative agreement. The difference between the calculated and measured values is discussed.

2010 Optical Society of America

OCIS codes: (060.4005) Microstructured Fibers; (060.2400) Fiber Properties; (060.2370) Fiber Optics Sensors.

References and links

1. J. Wang, and L. Wang, "Liquid-filled microstructured polymer fibers as monolithic liquid-core array fibers," Appl. Opt. **48**(5), 881–885 (2009).
2. T. Nasilowski, *et al*., "Sensing with photonic crystal fibers," Intelligent Signal Processing, WISP 2007 IEEE International Symposium on, 1–6, (Oct. 2007).
3. G. Vienne, *et al*., "Liquid core fibers based on hollow core microstructured fibers", Lasers and Electro-Optics, 2005. CLEO/Pacific Rim 2005. Pacific Rim Conference on, 551–555, (Aug. 2005).
4. F. M. Cox, A. Argyros, and M. C. J. Large, "Liquid-filled hollow core microstructured polymer optical fiber," Opt. Express **14**(9), 4135–4140 (2006).
5. C. J. S. De Matos, C. M. Cordeiro, E. M. Dos Santos, J. S. Ong, A. Bozolan, and C. H. Brito Cruz, "Liquid-core, liquid-cladding photonic crystal fibers," Opt. Express **15**(18), 11207–11212 (2007).
6. S. Yiou, P. Delaye, A. Rouvie, J. Chinaud, R. Frey, G. Roosen, P. Viale, S. Février, P. Roy, J. L. Auguste, and J. M. Blondy, "Stimulated Raman scattering in an ethanol core microstructured optical fiber," Opt. Express **13**(12), 4786–4791 (2005).
7. M. Lelek, F. Louradour, V. Couderc, P. Viale, S. Fevrier, J. L. Auguste, J. M. Blondy, and A. Barthelemy, "High sensitivity autocorrelator based on a fluorescent liquid core," Appl. Phys. Lett. **89**(6), 061117 (2006).
8. F. Zolla, G. Renversez, A. Nicolet, B. Kuhlmey, S. Guenneau, and D. Felbacq, *Foundations of Photonic Crystal Fibres*, (Imperial College Press, Coven Garden, London, 2005), Chap. 1.
9. P. Russell, "Photonic crystal fibers," Science **299**(5605), 358–362 (2003).
10. M. J. F. Digonnet, H. K. Kim, G. S. Kino, and S. Fan, "Understanding air-core photonic-bandgap fibers: Analogy to conventional fibers," J. Lightwave Technol. **23**(12), 4169–4177 (2005).
11. N. M. Litchinitser, and E. Poliakov, "Anitiresonant guiding microstructured optical fibres for sensing applications," Appl. Phys. B **81**(2-3), 347–351 (2005).
12. H. Leutz, "Scintillating Fibre," Nucl. Instrum. Methods Phys. Res. A **364**(3), 422–448 (1995).
13. T. O. White, "Scintillating Fibres," Nucl. Instrum. Methods Phys. Res. A **273**(2-3), 820–825 (1988).
14. G. F. Knoll, *Radiation Detection and Measurement*, (John Wiley & Sons, New York, 2000), Chap. 8,14.
15. C. Zorn, "A pedestrians guide to radiation damage in plastic scintillators," Radiat. Phys. Chem. **41**(1-2), 37–43 (1993).
16. Saint Gobian Liquid Scintillator Products, *http://www.detectors.saint-gobain.com/Liquid-Scintillator.aspx*.
17. CUDOS Multipole Analysis Software for Microstructured Fiber: http://*www.physics.usyd.edu.au/cudos/research/old%20site/pcf.html*.
18. FIMMWAVE from Photon Design: http://*www.photond.com*.
19. A. W. Snyder, and J. D. Love, *Optical Waveguide Theory*, (Chapman and Hall, New York, 1983) Chap. 1–6.
20. D. Gloge, "Weakly guiding fibers," Appl. Opt. **10**(10), 2252–2258 (1971).
21. J. J. Fitzgerald, G. L. Brownell, and F. J. Mahoney, *Mathematical Theory of Radiation Dosimetry*, (Gordon and Breach Science, New York, 1967), Chap. 5.
22. NIST x-ray absorption data for common materials: Plastic Scintillator (Vinyl toluene): *http://physics.nist.gov/PhysRefData/XrayMassCoef/ComTab/vinyl.html*.

1. Introduction

Liquid filled microstructured optical fiber (MOF) offers significant sensing and detection capability. It is considered for many sensing and detection applications [1–7]. Various liquids offer a broad range of unique sensing and detection applications.

Previous investigations of MOF, also known as photonic crystal fiber (PCF), show light guidance through 'leaky' evanescent modes [8]. An important aspect of band-gap and effective index fibers is the dependence of the guided wavelength on fiber geometry. For near infrared (IR) wavelengths, band-gap fibers operate through a narrow range of wavelengths; effective index fibers can have single mode operation over an extended wavelength range [9,10].

Filling the inclusions of the MOF changes the refractive index. At near IR wavelengths, fiber with a core index of refraction less than the cladding forms a band-gap or ARROW waveguide [11]. For shorter wavelengths, the waveguide modal characteristics change based on the material index of refraction and fiber geometry. Shorter wavelengths are investigated in this work.

For x-ray detection, ionizing radiation can be detected by using both plastic scintillating fibers and doped glass fibers [12,13]. Scintillation occurs as the absorption of shorter wavelength photons generates longer wavelength photons that are detected [14]. Although scintillation occurs in gases, liquids, and solids, liquids allow more convenient sensor fabrication based on previous MOF work [1–7].

We present an x-ray detecting fiber by filling MOF with a liquid scintillator which has several benefits compared to plastic scintillating fiber. Conventional plastic scintillating fiber operates with a large core and small cladding to reduce internal reflections which cause losses due to imperfections between the core-cladding interface [12]. Liquid filled microstructured fiber does not have these losses due to the step index between the liquid core and quartz cladding. The smaller diameter of the microstructured fiber allows coupling with standard multimode fiber using standard mechanical couplers. Additionally, the plastic fiber core gradually becomes opaque when exposed to x-rays over time while the liquid remains clear [12,15].

This paper describes how the MOF functions as a detector when exposed to x-rays and transmits light; it also shows how to calculate the maximum theoretical output and experimentally measure the output. Numerical modeling shows that light is confined in the liquid, which is verified in experiments using liquid filled MOF. The numerical modeling and experimental observations leads to a geometric optics waveguide model. Calculated output and experimental data are compared for a liquid filled MOF irradiated with a CdTe characterized 40kV x-ray source.

2. Numerical modeling and theory

The BC-517H liquid scintillator used emits 425 nm wavelength photons and was chosen because of its refractive index [16]. The propagation of light in microstructured fiber as shown in Fig. 1 was analyzed using a wavelength of 425 nm. The FIMMWAVE finite element solver and CUDOS multi-pole software package provided modal solutions for the fiber models shown in Fig. 2 [17,18].

The results from the FIMMWAVE and CUDOS models show all the effective refractive index solutions are real and all the modes are real and guided. These guided bound modes exist within the inclusions. Thus, numerical analysis results show the filled MOF operates as a bundle of index guiding fibers for light transmission at the 425 nm wavelength.

A small difference exists between the refractive indexes of the fiber silica matrix (n = 1.4585) and liquid filled inclusions (n = 1.476). This small refractive index difference allows using weakly guiding total internal reflection waveguide theory [19,20]. The inclusions are modeled as a bundle of weakly guiding multimode fibers with negligible mode coupling.

Considering the liquid MOF as multi-core fiber, evaluation of the normalized frequency V parameter shows multimode transmission

$$V = \left(2\pi\rho / \lambda\right)\left[n_i^2 - n_m^2\right]^{1/2} \qquad (1)$$

where ρ is the inclusion diameter and the subscripts i and m are for the inclusion and cladding matrix index of refraction, respectively. For a 425 nm wavelength with ρ = 2500nm, n_i = 1.476, n_m = 1.4585 yields V = 8.375 and each liquid filled inclusion is approximated as a step index multimode fiber [19]. The weakly guiding waveguide approximation is valid if $\Delta \ll 1$.

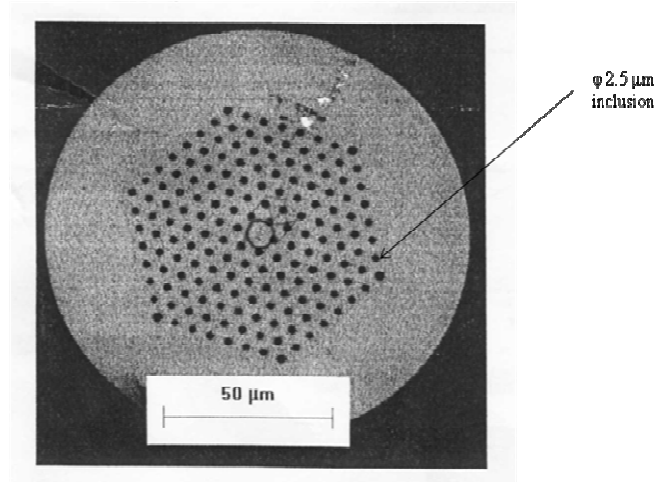$$\Delta = \left(n_i^2 - n_m^2\right) \Big/ 2n_i^2 \qquad (2)$$

Fig. 1. Microstructured quartz optical fiber cross-section. Total fiber diameter is 125 microns with 168 air filled inclusions. These inclusions become fiber cores when filled with scintillator material.
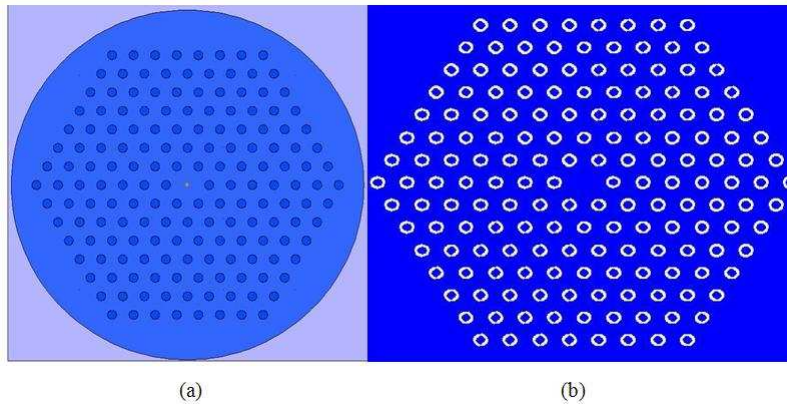

Fig. 2. (a) FIMMWAVE FEM model geometry, (b) CUDOS multipole model geometry. Note the center hole in the FIMMWAVE model is filled by using cladding material.

For the liquid and quartz, $\Delta \approx 1\%$, which satisfies the weakly guiding approximation. This allows analytical solutions from step index weakly guiding optical fiber theory [20]. The number of modes is given by N_m.

$$N_m \approx V^2 \Big/ 2 \qquad (3)$$

Considering the photons as rays from a spherical dipole, the complementary critical angle θ_c for guiding the photons is defined using

$$\Delta = \frac{1}{2} \sin^2 \theta_c \qquad (4)$$

where the complementary critical angle, θ_c, limits the angle of bound rays propagation in the fiber. The photon capture probability

$$P_{nc} = \frac{\int_0^{\theta_c} \sin(\varphi) d\varphi}{2} = \frac{1 - \cos(\theta_c)}{2} \qquad (5)$$

is the ratio of surface area emitted through θ_c to the total spherical surface area [20]. Using Eqs. (2) and (4) with Eq. (5) yields $P_{nc} = 0.59\%$. For multimode power transmission the percent of power guided through bound modes is [20, 21]

$$\eta_{wg} = \frac{P_{core}}{P} \approx 1 - \frac{4}{3\sqrt{N_m}} \qquad (6)$$

where P_{core} is the guided core power and P is the total power. Equations (1), (3), and (6) combine for a waveguide efficiency, $\eta_{wg} = 77\%$. The liquid scintillator has an output of 7.5/keV photon emission per absorbed gamma photon, which yields

$$N_P(E) = \left(7.5 \frac{photons}{keV}\right) EN(E) \qquad (7)$$

where E is the energy per x-ray photon in keV and N is the number of absorbed monochromatic x-ray photons per unit time. Beer's law

$$I = I_o e^{-\alpha l} \qquad (8)$$

relates the absorbed x-ray photon intensity to length l using an absorption coefficient α and $I = (h\nu)N/A$, where A is the area. The number of absorbed x-ray photons as a function of energy per unit time uses the intensity relation and Eq. (8) to yield

$$N(E) = A_r (1 - e^{-\alpha(E)l}) N_{count}(E) \qquad (9)$$

where $N_{count}(E)$ is the total number of x-ray photons at energy E, and $\alpha(E)$ is the absorption coefficient. A_r is the area ratio between the 100 micron diameter collimator and 168-2.5 micron diameter holes, $A_r = (168 \cdot 2.5^2)/100^2$ and l is the fiber length. The BC-517H absorption coefficient was approximated by vinyl toluene data [22].

The photomultiplier quantum, collection, and transmission efficiencies combine to an approximate detector efficiency $\eta_d = 18\%$. The maximum photomultiplier electrical pulse count rate during x-ray exposure of the liquid MOF is

$$N_c = \int N_P P_{nc} \eta_d \eta_{wg} dE \qquad (10)$$

where N_P is a function of energy given by Eq. (7), which uses Eq. (9).

3. Experiment and results

Sample fiber preparation was done by putting liquid scintillator into the MOF using capillary action along with pressurizing the liquid at one end of the fiber. A 12cm long fiber was chosen because that length has over 95% x-ray photon absorption for a 40keV x-ray. Figure 3. shows fiber photon emission generated by a UV lamp source during examination and testing

of fibers before exposure to x-rays. The inspection allowed determining fiber quality and confirming the theoretical modeling.

Conducting an experiment allowed measuring the fiber photon count during x-ray exposure for comparison with calculations. Measurements were taken between x-ray tube voltages of 10 and 40 kV at 5kV increments. A 40 kV, 4 W silver anode x-ray tube was the source. Figure 4 shows the experimental setup for x-ray tube characterization and scintillating fiber output measurements. The x-ray tube characterization used a collimated CdTe detector and multichannel analyzer.

The collimator had two 5 mm thick tungsten aperture disks, a 100 micron diameter aperture followed by a 200 micron diameter aperture. The CdTe detector operated at 100% efficiency for x-ray photons between the energies of 10-50 keV. The CdTe detector multichannel analyzer stored data on a computer for subsequent processing.
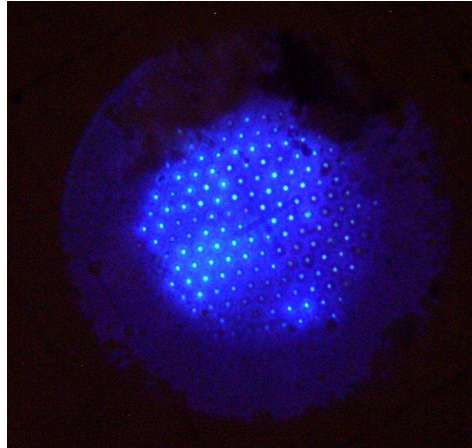

Fig. 3. Emission of 425 nm photons using UV excitation on opposite end of fiber; liquid loss from the fiber end results in no emission.
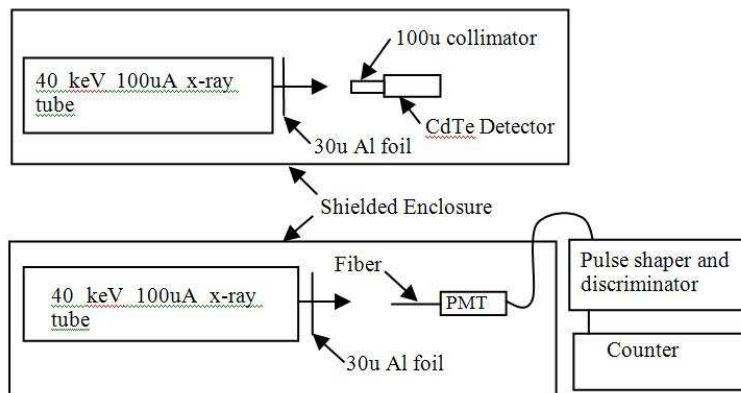

Fig. 4. Placement of CdTe detector and collimator for characterization of x-ray tube and taking fiber data.

The tube characterization progressed at five minute intervals over a series of weeks to ensure tube stability and measurement repeatability. The CdTe detector energy calibration used an Am-241 radioactive source. Careful alignment of the collimator and tube maximized photon counts through the collimator, which was located 0.5 cm from the tube.

A 1024 channel analyzer measured the number of x-ray photons (N_{count}) at discrete energies which pass through the 100 micron diameter collimator. The value of energy was

interpolated from a linear calibration scale. The photons counted from each channel formed the 1024 element array N_{count} (E) used in Eq. (9).

Signals from the photomultiplier tube went to a discriminator circuit, which discarded voltage pulses below an adjustable level. The remaining pulses went to a digital pulse counter where the counts accumulated over a 300 second period. The total pulse count was recorded at discrete x-ray tube voltages between 10 and 40 kV.

A blackout cloth was used over a leaded Plexiglas three-sided enclosure with a lead-foil covered aluminum back plate. The blackout cloth reduced stray photons and their subsequent noise but allowed easy access to the experimental setup. Additionally, the room was partially darkened during operation to remove fluorescent light fixture magnetic and photonic noise.

Lead shielding was wrapped around the photomultiplier tube module and fiber coupler to reduce noise. Power and cables to the photomultiplier tube and x-ray tube were routed between the Plexiglas enclosure and backing plate. Power for the electronics had a common ground.

The prepared fiber was placed in the same location as the detector collimator while varying x-ray tube voltage without changing source current during measurements. A bare fiber FC adapter coupled the fiber to the photomultiplier tube. The photomultiplier tube used a bialkali cathode with peak quantum efficiency at 420 nm. The fiber directed scintillation photons to the photomultiplier tube.

Figure 5. shows the calculated photon output with measured output. The calculated output uses Eq. (10) with x-ray tube characterization measured data used for N_{count}. Displayed counts have noise subtracted from their measured value.
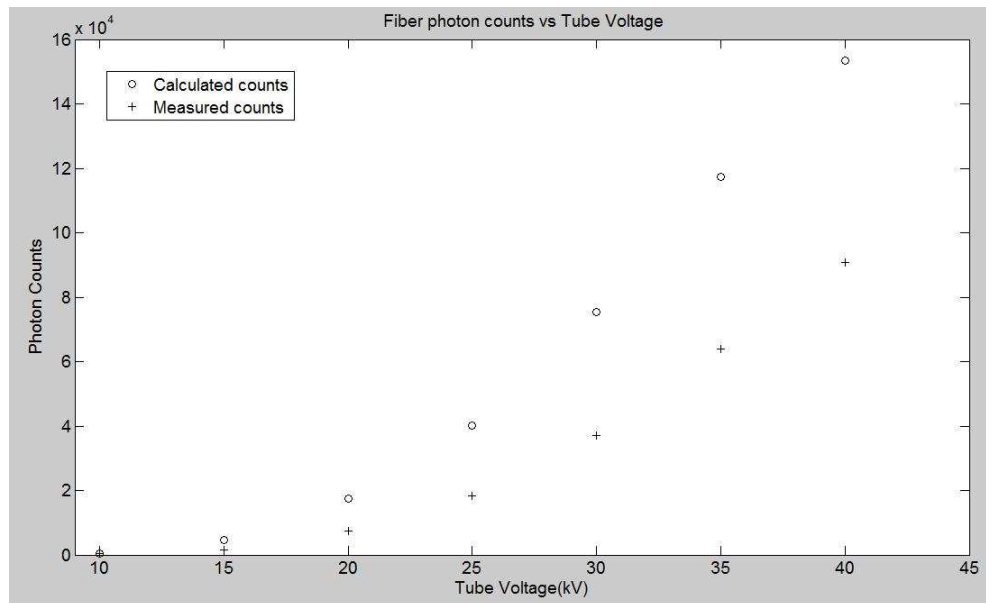

Fig. 5. Fiber photon counts versus tube voltage comparing calculated with measured counts.

4. Discussion and conclusions

The data shape and trend of Fig. 5. shows good agreement between the calculated and measured values. The primary contributors to the difference between the measured and calculated photon counts are the material x-ray absorption coefficient in the liquid, scattering, and lack of complete MOF end filling illustrated in Fig. 3.

Fiber alignment and orientation determine the x-ray absorption. These absorbed x-rays generate photon emission in the liquid. Considering the length of fiber used, attenuation through the liquid and coupling between cores is approximately negligible. Scattering effects

have been ignored in the theory and modeling. Scattering due to geometric and material non-uniformities will cause loss of transmitted light. Incompletely filled MOF results in almost no transmission due to scattering.

The geometric optics theory used for calculating the maximum photon counts is based on numerical analysis and experimental observations. The sample observations, shown in Fig. 3, confirm the numerical analysis. The short wavelength photons generated by x-ray absorption transform the liquid MOF into a multi-core x-ray detecting fiber.

The work presented shows liquid MOF can be used to measure x-rays. The x-ray detecting liquid MOF was observed to be highly direction sensitive. Making the exposed end of the fiber highly reflective will increase the measured photon count.